Dynamic Investigations of an Endogenous Business Cycle Model with Heterogeneous Agents

Spiros Bougheas
University of Nottingham

Pasquale Commendatore
University of Naples Federico II

Laura Gardini
University of Urbino Carlo Bo

Ingrid Kubin
Vienna University of Economics and Business
Corresponding author: ingrid.kubin@wu.ac.at

September 1, 2023

Abstract

We introduce agents' heterogeneity into a model of endogenous business cycles, in which agents can invest either in 'good' projects that contribute to future capital formation, or in 'bad' projects without that property. The resulting map involves three distinct regimes, two of which we linearize. Using theoretical results on piecewise linear systems and on border collision bifurcations, we are able to provide a thourough analysis of the dynamics.

Key Words: business cycles, heterogeneous agents, piecewise linear systems, bifurcations

JEL: C61, E32

1. Introduction

Matsuyama *et al.* (2016) offer an endogenous explanation of business cycles within a representative agent framework. In their model agents can invest either in 'good' projects whose output can either be consumed or invested, thus contributing to future capital formation, or in 'bad' projects that can only be consumed. Good projects are produced with a Neoclassical production function that is subject to diminishing returns while the return of bad projects is constant. Thus, as the economy grows and the return of good projects drops below that of bad projects entrepreneurs have incentives to invest in the latter. However, investment in bad projects is financially constrained. Provision of funds for such investment depends on the entrepreneur's net worth. Thus, even if the stage of development of the economy is such that the return of bad projects is higher than that

of good projects, financial constraints might limit the investment in bad projects. Under these conditions the economy can exhibit complex dynamics that include both periodic and aperiodic fluctuations. Along a typical two-period cycle when the level of capital/labor ratio, and thus net worth, is too low for any funds to be allocated to bad projects, some of the output of good projects will be devoted to capital formation and thus the following period there will be a higher capital/labor ratio. But now the financial constraints are relaxed and as entrepreneurs invest in bad projects capital formation declines and the following period the capital/labor ratio drops and a new cycle begins.

In this paper, we extend the basic framework and allow for heterogeneous agents, which differ in their initial endowment. In this framework, interesting new questions can be studied. For example, in financial economics there are two types of credit rationing. There are some agents that cannot obtain funds at all and therefore cannot become entrepreneurs, while others might be able to get some funds but below the optimal level and therefore will underinvest. These two margins of adjustment for investements (who is going to invest and how much) will be in the focus of our analysis. In addition, this framework can be used to help us understand how financial constraints affect occupational choice (entrepreneurship) along the different phases of the business cycle. The model can also be applied to the study of the effects of business cycles on income inequality. However, the introduction of heterogeneous agents involving two margins of adjustment complicates significantly the analytics of dynamic solutions. In this paper we provide extensive analytical results for a linearized version of the model that can complement other numerical approaches (reviewed below). We focus our analysis on the nature of the business cycles, its severity and duration, and on the regime switches that are involved. We show how the introduction of heterogeneity affects the impact of financial constraints on the characteristics of the business cycle.

The mathematical form of the model is a one-dimensional piecewise smooth and continuous system in discrete time, with two kink points at which the map changes its definition. These kink points have a clear economic motivation and reflect the fact that investment in bad projects is financially constrained. They play an important role for the resulting dynamics. We describe, in five propositions, which kind of attracting sets can occur and the related bifurcations. The analysis is performed by using much of the theory of piecewise smooth systems and in particular piecewise linear systems, that is nowadays enough developed (see Avrutin *et al.*, 2019, and the references therein), and uses the border collision bifurcations to explain many of the changes that may occur. In fact, in piecewise smooth systems, the bifurcations are often not the usual ones occurring in smooth systems, and the classification of the possible dynamics may be quite different, involving the kink points of the system.

Our paper is related to a number of papers that extend Matsuyama (2013). Matsuyama et al. (2016) is a simpler version of Matsuyama (2013) that allows for a richer menu of technologies. The slightly simpler version in Matsuyama *et al.* (2016) allows for a more detailed study of the stability properties of the model. Other studies that use this framework to examine issues related to business cycles are Bougheas *et al.* (2022), Kubin and Zörner (2021) and Kubin *et al.* (2019). Bougheas *et al.* (2022), motivated by events in financial markets around the Global Financial Crisis of 2008, introduces a banking sector

that has a choice between financing productive projects and investing funds in high yield investments that do not contribute in capital formation. As in the present paper agents are heterogeneous which allows the authors to study income inequality dynamics along the business cycle. In contrast to the present paper, the whole analysis is performed on the non-linearized version and, thus, some of the results are obtained numerically. Kubin and Zörner (2021) augment Matsuyama *et al.* (2016) by introducing human capital and study the effects of learning-by-producing on the evolution and stability of income distribution, while Kubin *et al.* (2019) take aspects from behavioral finance on board.

The rest of the paper is organized as follows. In Section 2, we motivate and describe the model which extends Matsuyama et al. (2016) by allowing for borrowing and lending among heterogeneous agents. As we mentioned above, heterogeneity of agents introduces a second margin of adjustment for investment. Under a representative agent, like in Matsuyama et al. (2016), only the level of investment matters which simplifies the model and allows for the derivation of closed form solutions. The reason is that after the second kink the map is a straight line with zero slope. However, when heterogeneity is introduced, as in the banking model of Bougheas et al. (2022) both margins adjust which complicates considerably the analysis of the model. Now after the second kink the map is non-linear and upward sloping implying that only computational solutions are feasible. In Section 3 we present a linearized version of the model that can be analytically solved. We focus our analysis on the interaction between financial constraints and the nature of business cycles (how strong are the fluctuations of capital and output per capita? how long are business cycles? and which regime switches do they involve?) and leave other applications to further research. Finally, section 4 summarizes some results evidencing their role in the economic context and pointing to possible future extensions.

2. The Model

Time is discrete and the horizon infinite ($t = 0, 1, 2, ...$). At each date a generation of unit mass is born and lives for two periods. Young agents born at t are not homogeneous. They are endowed with z units of (effective) labor that they supply inelastically for the production of the final good. The distribution of labor endowments is continuous, time invariant with support on $[z, \bar{z}]$ and density function $g(z)$. Let $\hat{z}$ denote the level of aggregate (average) endowments. We normalize the aggregate supply of labor to 1. Young agents do not consume.

The single final good can be produced by two distinct technologies. One is a constant returns-to-scale technology, $y_t = f(k_t)$ where y_t denotes per capita output and k_t denotes the capital/labor ratio at t. For all t, $f'(k_t) > 0 > f''(k_t)$, $f(0) = 0$ and $f'(0) = \infty$. The final good can either be consumed or invested (good projects). Capital fully depreciates in one period. Factor markets are competitive with the reward to physical capital equal to $\rho_t = f'(k_t)$, and the reward to labor equal to $w_t = f(k_t) - k_t f'(k_t) \equiv W(k_t) > 0$. Thus, the labor income of a young agent with endowment z is equal to $zW(k_t)$. The second technology uses only capital with each unit of capital yielding B units of the final good. The output of this technology cannot be invested (bad projects).

At the end of the first period (the beginning of the second period), young agents have

received their wage income and turn old. They have the following two options. One option is to become lenders by investing their endowments in frictionless competitive financial markets and enjoy a utility benefit u (home production or leisure). The other option is to become entrepreneurs by using their endowments together with borrowed funds to invest in the good projects technology. The amount of the final good that agents can borrow from the financial system depends on their endowments. AT t, an agent with endowment z will be able to borrow a maximum amount of $(m-1)zw_{t-1}$ units of the final good from financial markets (total investment in good projects will be equal to mzw_{t-1}, where $m > 1$).[1]

Financial markets can use the funds invested by lenders either to offer funds to entrepreneurs or to invest in bad projects. However, the latter type of investment is constrained. To ensure consistency with Matsuyama *et al.* (2016), we assume that bad projects become gradually available after the economy reaches a certain level of development.[2] Let $\hat{V}(k_t)$ denote the level of bad projects available and $V(k_{t+1})$ denote the funds invested in bad projects. Let r_t denote the market clearing interest rate.

An agent with endowment z, if he chooses to produce good projects will earn income $f'(k_{t+1})zmw_t$, repay $r_{t+1}(m-1)zw_t$ to the financial market and consume the difference. The same agent, if he chooses to invest in the financial market, will consume $r_{t+1}zw_t$. Thus, as long as,

$$f'(k_{t+1})zmw_t - r_{t+1}(m-1)zw_t \geqslant r_{t+1}zw_t + u \tag{2.1}$$

an agent endowed with z units of labor will invest in good projects. Let z_t^* denote the level of endowment such that the agent is indifferent between the two options.

Market clearing in financial markets requires that

$$\int_{z_{t+1}^*}^{\bar{z}} (m-1)zw_t g(z)dz + V(k_{t+1}) = \int_{\underline{z}}^{z_{t+1}^*} zw_t g(z)dz \tag{2.2}$$

The evolution of the capital/labor ratio will depend on whether or not there is investment in bad projects and if there is such investment whether or not is constrained. The exact form will be given below.

Bad Projects Are Not Available For sufficient low levels of the capital/labor ratio bad projects will not be available. In this case, $V_{t+1} = 0$, and the capital/labor ratio at $t+1$ is given by wages at t:

$$k_{t+1} = mW(k_t) \equiv F(k_t). \tag{2.3}$$

---

[1]With heterogeneus agents the financial constraint avoids corner solutions where all funds would have been lent to the agent with the highest endowment.

[2]One way to interpret the model is that investments in financial markets can take the form of bonds to corporations or CDOs. The first type of investment is more likely to enhance capital formation. Furthermore, it is also reasonably to assume that derivatives are more likely to be offered by well-developed financial markets.

Investment In Bad Projects Is Unconstrained Arbitrage will force the interest rate to be equal to the return of bad projects, $r_{t+1} = B$. Then, from (2.1) holding with equaity we have

$$z^*_{t+1} = \frac{u}{W(k_t)\left(f'(k_{t+1}) - B\right)m}. \tag{2.4}$$

The evolution of capital is

$$k_{t+1} = \int_{z^*_{t+1}}^{\bar{z}} mzW(k_t)g(z)dz \tag{2.5}$$

(2.4) and (2.5) together solve for k_{t+1} and z^*_{t+1}. We write the solution for the evolution of the capital/labor ratio as

$$k_{t+1} \equiv H(k_t). \tag{2.6}$$

with $H'(k_t) > 0$.

To prove this, rearranging (2.4) we have

$$f'(k_{t+1}) = B + \frac{u}{z^*_{t+1} \cdot W(k_t) \cdot m} \tag{2.7}$$

and from (2.5) we can write

$$k_{t+1} = \int_{z^*_{t+1}}^{\bar{z}} mzw_t g(z)dz = W(k_t) \cdot m \cdot \int_{z^*_{t+1}}^{\bar{z}} zg(z)dz \tag{2.8}$$

The two equations in (2.7) and (2.8) form a system with z^*_{t+1} and k_{t+1} as variables, given k_t and the parameter B, u and m. Taking the total derivative with respect to k_{t+1}, z^*_{t+1} and k_t of (2.7) results in

$$dk_{t+1} = Z1 \cdot dz^*_{t+1} + W1 \cdot dk_t \tag{2.9}$$

where $Z1 = \frac{-u}{mW(k_t)\left(z^*_{t+1}\right)^2} \frac{1}{\frac{d^2 f(k_{t+1})}{dk^2_{t+1}}} > 0$ and $W1 = \frac{-u}{m(W(k_t))^2 z^*_{t+1}} \frac{\frac{dW(k_t)}{dk_t}}{\frac{d^2 f(k_{t+1})}{dk^2_{t+1}}} > 0$.

The total derivative of (2.8) is

$$dk_{t+1} = Z2 \cdot dz^*_{t+1} + W2 \cdot dk_t \tag{2.10}$$

where $Z2 = -mW(k_t) z^*_{t+1} g(z^*_{t+1}) < 0$ and $W2 = \frac{dW(k_t)}{dk_t} \cdot m \cdot \int_{z^*_{t+1}}^{\bar{z}} zg(z)dz > 0$.

Solving (2.9) and (2.10) results in

$$\frac{dk_{t+1}}{dk_t} = \frac{W2Z1 - W1Z2}{Z1 - Z2} = SlopeH > 0 \tag{2.11}$$

Investment In Bad Projects Is Constrained From (2.2) we have

$$\hat{z} = m\int_{\hat{z}_{t+1}}^{\bar{z}} zg(z)dz + \frac{V(k_t)}{W(k_t)} \tag{2.12}$$

Further, due to the constraint, the evolution of the capital/labor ratio is given by

$$k_{t+1} = \left(W(k_t) - \hat{V}(k_{t+1})\right) \equiv G(k_t). \tag{2.13}$$

5

3. The dynamics of the model

3.1. Functional forms

The resulting map (see Fig.1) has three branches and involves two thresholds that are the points of intersection between the functions F and G and between G and H, also called kink points, where the map changes its definition with continuity: k^{FG} and k^{GH}:

$$k_{t+1} = \begin{cases} F(k_t) & \text{if} \quad 0 \leq k_t \leq k^{FG} \\ G(k_t) & \text{if} \quad k^{FG} < k_t < k^{GH} \\ H(k_t) & \text{if} \quad k^{GH} \leq k_t \end{cases} \qquad (3.1)$$

For the dynamic analysis, we specify the following functional forms:

1. We use $F(k_t) = C\sqrt{k_t}$, where C is a parameter.

2. Without strong alternatives, we assume a linear specification for $G(k_t)$

$$G(k_t) = \delta(k_t - k^{FG}) + F(k^{FG})$$

with k^{FG} and δ as parameters.

There are a couple of alternative economic interpretations of these two parameters. In Matsuyama et al. (2016) investment in bad projects is financially constrained. The representative agent's wealth (measured by per capita capital) must reach a certain threshold value, captured by k^{FG}, before agent's can borrow funds to invest in bad projects. Then, the value of δ captures how fast these constraints are relaxed. In Bougheas et al. (2022) banks invest in bad projects and their availability depends on the level of financial innovation. In turn, it takes a certain level of economic development, captured by the threshold value k^{FG}, before financial innovation takes off. Then, the value of δ captures the speed of financial innovation. Below we assume that $\delta < 0$ reflecting a relatively fast availability of bad projects, implying a substitution of bad for good projects for $k_t > k^{FG}$.

3. We also linearize $H(k_t)$ based on the following two observations:

First, there exists a threshold for the capital stock k^{FH}, beyond which bad projects are more profitable than good projects and

Second, the adjustment along the two margins implies that capital invested in good projects increases even if investment in bad projects is unconstrained, we introduce the parameter $\varepsilon > 0$ to capture this effect. At the same time, investment in bad projects imply that $\varepsilon < 1$. Assuming that the first effect exists, but is not very strong, leads to $0 < \varepsilon << 1$. Thus, we use:

$$H_l(k_t) = \varepsilon(k_t - k^{FH}) + F(k^{FH}) \qquad (3.2)$$

with k^{FH} and ε as parameters.
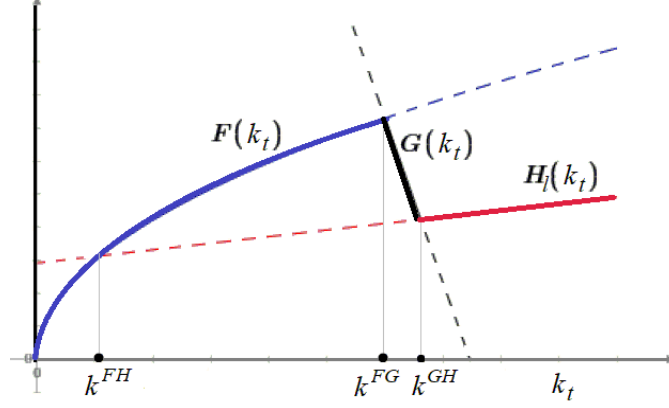
Fig.1 Map $k_{t+1} = T(k_t)$

The analysis proceeds with this system $k_{t+1} = T(k_t)$:

$$T(k_t) := \begin{cases} F(k_t) = & C\sqrt{k_t} & \text{if} & 0 \le k_t \le k^{FG} \\ G(k_t) = & \delta(k_t - k^{FG}) + F(k^{FG}) & \text{if} & k^{FG} < k_t < k_{GH} \\ H_l(k_t) = & \varepsilon(k_t - k^{FH}) + F(k^{FH}) & \text{if} & k^{GH} \le k_t \end{cases} \qquad (3.3)$$

where k^{GH} denotes the intersection point of the two straight lines $G(k_t)$ and $H_l(k_t)$. We summarize the conditions on the five parameters:

$$C > 0, \ k^{FG} > 0, \ k^{FH} \in (0, k^{FG}), \ \delta < 0, \ 0 < \varepsilon << 1 \qquad (3.4)$$

For the sake of notational convenience, we define

$$N_G = [C\sqrt{k^{FG}} - \delta k^{FG}] \ , \quad N_H = [C\sqrt{k^{FH}} - \varepsilon k^{FH}] \ , \quad k^{GH} = \frac{1}{\varepsilon - \delta}[N_G - N_H] \qquad (3.5)$$

so that we have the one-dimensional map

$$k_{t+1} = T(k_t), \quad T(k_t) = \begin{cases} F(k_t) = & C\sqrt{k_t} & \text{if} & k_t \le k^{FG} \\ G(k_t) = & \delta k_t + N_G & \text{if} & k^{FG} < k_t < k^{GH} \\ H_l(k_t) = & \varepsilon k_t + N_H & \text{if} & k^{GH} \le k_t \end{cases} \qquad (3.6)$$

that is continuous and piecewise smooth with two kink points (k^{FG} and k^{GH}) at which the map changes its definition. Map T has a maximum in the point k^{FG}, given by $F(k^{FG}) = C\sqrt{k^{FG}}$, and the iteration on the positive axis $k_t \ge 0$ are mapped into the interval $[0, C\sqrt{k^{FG}}]$, so that the map is bounded. We mention here that the fixed point $k^* = 0$ always exists and is repelling, and we do not consider it further, since the trajectory of points on the right side of $k^* = 0$ are mapped into an absorbing interval.

Note that the model - although similar in spirit to Matsuyama *et al.* (2016) - is different from an analytical perspective: Matsuyama *et al.* (2016) use a more general specification of the F function; in their model, linearity of the G function is a special case; and their H function is always horizontal, whereas in our case by introducing heterogeneity, it has a positive slope. Finally, our analysis focuses on the role of different parameters. We study

7

how the availability of bad projects affects the dynamics. In the map, this is reflected by the properties of the G function, namely by k^{FG} and δ. We are interested in the symbolic sequences on the cycles. In addition, we are interested in the implications of the heterogeneity and the two margins of adjustment. In the map, this is reflected by the (positive) slope of the H_l function, i.e. by the parameter ε.

3.2. Dynamic properties

In this section we focus on how the availability of investments in bad projects affects the asymptotic dynamics; the related parameters are k^{FG} and δ. In a first, more technical step we determine the possible equilibria of the model, the related bifurcations, and the conditions under which the map can be ultimately delimited in some absorbing interval involving only two branches of the map or all the three branches.

For $T(k^{FG}) < k^{FG}$ the map has the only fixed point related to the function F, given by $k_F^* = C^2$.

For $T(k^{FG}) > k^{FG}$ and $T(k^{GH}) < k^{GH}$ the map has the only fixed point $k_G^* = \frac{N_G}{1-\delta}$ related to the function G while for $T(k^{GH}) > k^{GH}$ the map has the only fixed point $k_H^* = \frac{N_H}{1-\varepsilon}$ related to the function H_l. When the condition $T(k^{FG}) = k^{FG}$ holds, it is the border collision of the two fixed points with the first kink point, $k_F^* = k_G^* = k^{FG}$, while when $T(k^{GH}) = k^{GH}$ holds, it is the border collision of the two fixed points with the second kink point, $k_G^* = k_H^* = k^{GH}$.

Since $\varepsilon < 1$ the last branch of the map, related to the function H_l either is below the diagonal (for $T(k^{GH}) < k^{GH}$), or it leads to the globally attracting fixed point k_H^* (for $T(k^{GH}) > k^{GH}$) where globally means for any $k_t > 0$.

For $T(k^{GH}) > k^{GH}$, that is, for $\varepsilon k^{GH} + N_H > k^{GH}$ leading to

$$(1 - \varepsilon)N_G < (1 - \delta)N_H \tag{3.7}$$

we have the range

$$k^{FG} < \widetilde{k}^{FG} := \frac{1}{4\delta^2}\left(C - \sqrt{C^2 - 4\delta\frac{1-\delta}{1-\varepsilon}N_H}\right)^2 \tag{3.8}$$

or also

$$\delta < \frac{C(1-\varepsilon)\sqrt{k^{FG}} - N_H}{(1-\varepsilon)k^{FG} - N_H} \tag{3.9}$$

in which the fixed point x_H^* exists and is globally attracting. We can so define the curve of border collision (at which $k_G^* = k_H^* = k^{GH}$) :

$$\phi_H: \quad k^{FG} = \widetilde{k}^{FG} \text{ or } \delta = \frac{C(1-\varepsilon)\sqrt{k^{FG}} - N_H}{(1-\varepsilon)k^{FG} - N_H} \tag{3.10}$$

For $T(k^{FG}) < k^{FG}$, that is, for $k^{FG} > C^2$, the fixed point $k_F^* = C^2$ exists and is globally attracting, since the slope of F in the fixed point is $1/2$, and we can define the curve of border collision (at which $k_F^* = k_G^* = k^{FG}$) :

$$\phi_F: \quad k^{FG} = C^2 \tag{3.11}$$

8

For parameters such that $k^{FG} < k^*_G = \frac{N_G}{1-\delta} < k^{GH}$ (or equivalently for parameters between the two curves ϕ_H and ϕ_F) the fixed point $k^*_G = \frac{N_G}{1-\delta}$ exists, and for $-1 < \delta < 0$ it is globally attracting (since it attracts all the points between the two kink points, k^{FG} and k^{GH}, and from outside a trajectory must enter that interval). At $\delta = -1$ it undergoes a degenerate flip bifurcation (for the degenerate bifurcations see Sushko and Gardini, 2010), the result of which depends on the parameters of the other two functions of the map. If the fixed point k^*_G is closer to k^{FG} (than to k^{GH}) then at the bifurcation value the segment $[F^2(k^{FG}), F(k^{FG})]$ is filled with cycles of period 2, the last of which $\{F^2(k^{FG}), F(k^{FG})\}$ also undergoes a border collision bifurcation, and since the slope of the function F at the kink point k^{FG} is smaller than 1, the result of the bifurcation, for $\delta < -1$ is an attracting 2-cycle with periodic points in the F and G branches. Similarly, if the fixed point k^*_G is closer to k^{GH} (than to k^{FG}) then at the bifurcation value the segment $[H_l(k^{GH}), H_l^2(k^{GH})]$ is filled with cycles of period 2, the last of which $\{H_l(k^{GH}), H_l^2(k^{GH})\}$ also undergoes a border collision bifurcation, and since the slope of the function H_l at the kink point k^{GH} is smaller than 1, the result of the bifurcation, for $\delta < -1$ is an attracting 2-cycle with periodic points in the G and H_l branches. We have so proved the following

Proposition 1 *Existence and stability properties of the fixed points.*

(i) For $k^{FG} > C^2$ the fixed point $k^*_F = C^2$ is globally attracting. A border collision occurs at the curve ϕ_F (given in (3.11)).

(ii) For $\delta < \frac{C(1-\varepsilon)\sqrt{k^{FG}} - N_H}{(1-\varepsilon)k^{FG} - N_H}$ (or equivalently $k^{FG} < \frac{1}{4\delta^2}\left(C - \sqrt{C^2 - 4\delta\frac{1-\delta}{1-\varepsilon}N_H}\right)^2$) the fixed point $k^*_H = \frac{N_H}{1-\varepsilon}$ is globally attracting. A border collision occurs at the curve ϕ_H (given in (3.10), (3.8)).

(iii) For $\frac{1}{4\delta^2}\left(C - \sqrt{C^2 - 4\delta\frac{1-\delta}{1-\varepsilon}N_H}\right)^2 < k^{FG} < C^2$ the only fixed point is $k^*_G = \frac{N_G}{1-\delta}$, globally attracting for $-1 < \delta < 0$. A degenerate flip bifurcation occurs at $\delta = -1$, leading to an attracting 2-cycle.

These regions in the parameter plane (δ, k^{FG}) lead to areas that are illustrated in different colors in Fig.2(a) The global stability of the fixed points is shown in different yellow tonalities (bounded by the curves ϕ_H, ϕ_F and $\delta = -1$).
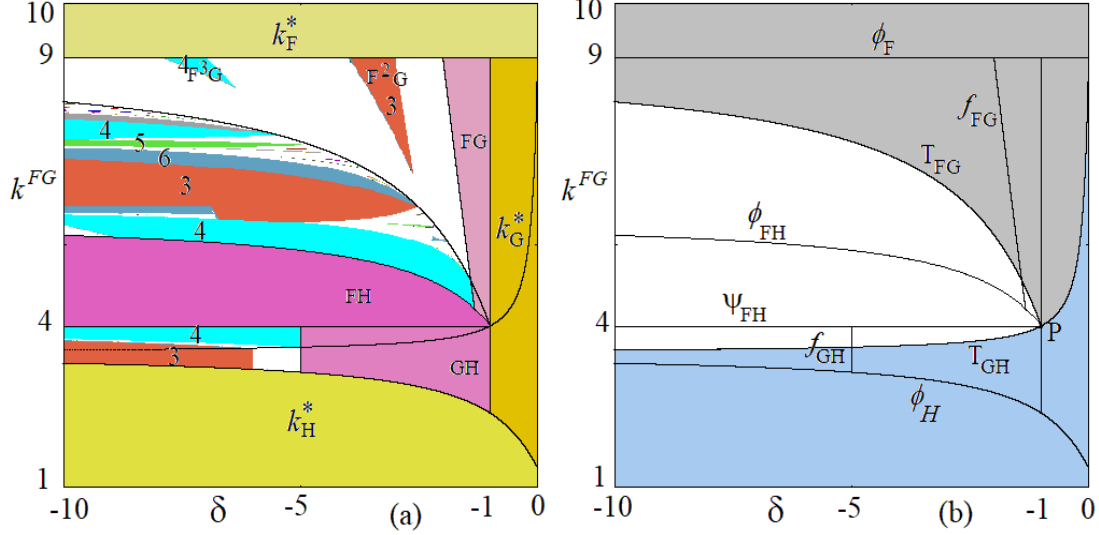
Fig.2 Two dimensional bifurcation diagram in the parameter plane (δ, k^{FG}) for $C = 3$, $k^{FH} = 1$ and $\varepsilon = 0.2$. In (a) the fixed points and the 2-cycles have regions in yellow and pink, respectively, with different tonalities, depending on the symbolic sequence. Red color corresponds to a 3-cycle, azure color to a 4-cycle, green color to a 5-cycle, while white regions correspond to chaotic intervals. In (b) the bifurcation curves are shown, and in the gray (resp. light blue) region the interval I_{FG} (resp. I_{GH}) is absorbing, in the white region the interval J is related to three branches of map T

For $k^{FG} > C^2$ the fixed point k_F^* is globally attracting. The border collision bifurcation occurring at $k^{FG} = C^2$ will be commented below. So we consider the case $k^{FG} < C^2$ to determine the existing absorbing interval. This will also clarify the kind of 2-cycle appearing at the bifurcation $\delta = -1$. As remarked above, the degenerate flip bifurcation of the fixed point k_G^* leads to an attracting 2-cycle, and which one depends on the value of the other parameters. Before commenting the point (say P) on the line $\delta = -1$ leading to the two different dynamic results, we look for the regions of the parameters related to the absorbing intervals that the map can have. In fact, the asymptotic trajectories can belong to an absorbing interval with two branches only (F and G or G and H_l), reducing to a unimodal map, or including all the three functions, so being characterized by a bimodal map. We have the following

Proposition 2 *Absorbing intervals. Let $k^{FG} < C^2$.*

(i) For $\delta > \frac{\varepsilon[k^{FG} - C\sqrt{k^{FG}}]}{(1-\varepsilon)k^{FG} - N_H}$ the interval $I_{GH} = [T(k^{GH}), T^2(k^{GH})]$ is invariant and absorbing, only the two branches with functions G and H_l are involved (azure region in Fig.2(b)).

(ii) For $\frac{(1-\varepsilon)C\sqrt{k^{FG}} - N_H}{k^{FG} - C\sqrt{k^{FG}}} < \delta < \frac{\varepsilon[k^{FG} - C\sqrt{k^{FG}}]}{(1-\varepsilon)k^{FG} - N_H}$ the interval $I_{FG} = [T^2(k^{FG}), T(k^{FG})]$ is invariant and absorbing, only the two branches with functions F and G are involved (gray region in Fig.2(b)).

(iii) For the remaining parameter points the interval $J = [T(k^{GH}), T(k^{FG})]$ is invariant and absorbing, all the three branches, with functions F, G and H_l, are involved (white region in Fig.2(b)).

10

Proof. As long as it is $T(k^{GH}) \geq k^{FG}$ then only the two branches with functions G and H_l are involved in the absorbing interval, so that the interval $I_{GH} = [T(k^{GH}), T^2(k^{GH})]$ is invariant and absorbing. While for $T(k^{GH}) < k^{FG}$ the absorbing interval of the map is $J = [T(k^{GH}), T(k^{FG})]$ and a smaller invariant interval $I_{FG} = [T^2(k^{FG}), T(k^{FG})] \subset J$ exists when it holds $T(k^{FG}) \leq k^{GH}$, inside which the map involves only the two functions F and G. While for $T(k^{FG}) > k^{GH}$ the smallest absorbing interval is J, involving all the three branches of the map. Notice that the interval $J = [T(k^{GH}), T(k^{FG})]$ is absorbing because the map is increasing below it (for $x_t < T(k^{GH})$) and decreasing above it (for $x_t > T(k^{FG})$), so that the trajectory of any point is mapped in J in a finite number of iterations (and the trajectory cannot escape from J). Similarly, when a smaller invariant absorbing interval exists (I_{FG} or I_{GH}) then the trajectory of any point is mapped in it in a finite number of iterations. The dynamics of the map in the smaller absorbing interval I_{GH} is topologically conjugate to that of the skew tent map (since it is piecewise linear, we refer to Sushko *et al.*, 2015, and Avrutin *et al.*, 2019 for the related dynamics and bifurcations), while the map in the smaller absorbing interval I_{FG} is unimodal and piecewise smooth, however, the border collision bifurcations related to the kink point k^{FG} may be studied by using the skew tent map as a border collision normal form.

The transition of the dynamics from the invariant interval I_{GH} to a different one occurs when the interval has a contact with the kink point k^{FG}. Considering the equality $T(k^{GH}) = k^{FG}$ we have

$$\frac{\delta}{\varepsilon - \delta}[N_G - N_H] + N_G - k^{FG} = 0$$

from which

$$T_{GH}: \quad \delta = \frac{\varepsilon[k^{FG} - C\sqrt{k^{FG}}]}{(1 - \varepsilon)k^{FG} - N_H} \tag{3.12}$$

The set T_{GH} so obtained is shown in Fig.2, below it the absorbing interval of the map is I_{GH} and involves only two branches, G and H_l. This proves point (i).

For $T(k^{GH}) < k^{FG}$, as long as it is $T(k^{FG}) \leq k^{GH}$ the absorbing interval is I_{FG}, so let us define the condition at which it holds $T(k^{FG}) = k^{GH}$. This condition leads to

$$C\sqrt{k_{FG}} = \frac{1}{\varepsilon - \delta}[N_G - N_H]$$

that is

$$T_{FG}: \quad \delta = \frac{(1 - \varepsilon)C\sqrt{k^{FG}} - N_H}{k^{FG} - C\sqrt{k^{FG}}} \tag{3.13}$$

The set T_{FG} so obtained is shown in Fig.2, above it the absorbing interval of the map is I_{FG}. This proves point (ii), and point (iii) is a consequence of (i) and (ii) □

We end now the comments related to the bifurcations of the fixed points, in the following

Proposition 3 *Bifurcations of the fixed points.*
(i) Let $P = (-1, k_P^*)$, where

$$k_P^* = \frac{1}{4}\left(\varepsilon C + \sqrt{(\varepsilon C)^2 + 4N_H}\right)^2 \tag{3.14}$$

11

then the degenerate flip bifurcation of the fixed point k_G^* occurring at $\delta = -1$ for $k^{FG} < k_P^*$ (resp. $k^{FG} > k_P^*$) leads to an attracting 2-cycle with periodic points in the two branches G and H_l (resp. F and G).

(ii) Crossing the border collision curve ϕ_F (given in (3.11)) from above ($k^{FG} > C^2$) to below ($k^{FG} < C^2$) the result of the border collision of the fixed point k_F^* depends on the value of the parameter δ. For $-1 < \delta < 0$ a persistence border collision occurs, leading to the globally attracting fixed point k_G^*; for $-2 < \delta < -1$ it leads to an attracting 2-cycle with periodic points in the two branches F and G; for $\delta < -2$ we can have transition to chaotic intervals or to attracting cycles of period 3, 4, 5.

(iii) Crossing the border collision curve ϕ_H (given in (3.10), (3.8)), from below ($k^{FG} < \widetilde{k}^{FG}$) to above ($k^{FG} > \widetilde{k}^{FG}$) the result of the border collision of the fixed point k_H^* depends on the value of the parameter δ. For $-1 < \delta < 0$ a persistence border collision occurs, leading to the globally attracting fixed point k_G^*; for $-1/\varepsilon < \delta < -1$ it leads to an attracting 2-cycle with periodic points in the two branches G and H_l; for $\delta < -1/\varepsilon$ we can have a transition to chaotic intervals or to attracting cycles of higher period, depending on the values of the two parameters ε and δ.

Proof. (i) Considering the flip bifurcation of the fixed point k_G^* for $\delta = -1$ both the conditions in (3.12) and in (3.13) lead to the same equation for k^{FG}, that is:

$$k^{FG} - \varepsilon C \sqrt{k^{FG}} - N_H = 0 \qquad (3.15)$$

from which we get the value k_P^* in (3.14), and the conditions $T(k^{GH}) = k^{FG}$ and $T(k^{FG}) = k^{GH}$ correspond to the existence of a 2-cycle with the two kink points $\{k^{FG}, k^{GH}\}$. That is, the two curves labelled T_{FG} and T_{GH} are intersecting in the point $P = (-1, k_P^*)$ on the bifurcation line $\delta = -1$. It follows that below (resp. above) the point P, the flip bifurcation of k_G^* leads to an attracting 2-cycle with periodic points in the two branches G and H_l (resp. F and G).

For (ii) the result of the border collision (for $k_F^* = k_G^* = k^{FG}$) only depends on the two slopes of the functions at the two sides of the fixed point. The slope of the function F at the border collision for $k_F^* = k^{FG}$ is fixed at $1/2$, while the slope of the function G is δ, so that for $-1 < \delta < 0$ it leads to persistence of attracting fixed point (k_G^* in the middle branch), when the product of the two slopes satisfies $-2 < \delta < -1$ the bifurcation leads to an attracting cycle of period 2, ad so on, the value of δ completely determine the result of the bifurcation (see Sushko *et al.*, 2015, and Avrutin *et al.*, 2019).

For (iii) the reasoning is similar, it occurs as for the border collision of the fixed point in the skew tent map, The slopes of the functions H_l and G at the border collision (for $k_G^* = k_H^* = k^{GH}$) are ε (< 1) and δ, so that for $-1 < \delta < 0$ it leads to persistence of attracting fixed point k_G^*, for $-1/\varepsilon < \delta < -1$ the bifurcation leads to one attracting 2-cycle with symbolic sequence GH, while for $\delta < -1/\varepsilon$ we can have chaotic intervals or other attracting cycles.□

In Fig.2(a) we can see the result of the flip and border collision bifurcations commented above in the parameter plane (δ, k^{FG}). Note that the figure illustrates the analytic result for specific parameter values. However, the equations of the bifurcation curves are analytically derived, and can be drawn for different constellations of the remaining parameters.

Each point (δ, k^{FG}) denotes the result of the asymptotic behavior of the map at the specific values for the parameters. Recall that in the blue region of Fig.2(b) related to a piecewise linear unimodal map in the absorbing interval I_{GH} then the attracting set is necessarily unique. In the gray region of Fig.2(b) related to a piecewise smooth unimodal map in the absorbing interval I_{FG} in general the attracting set may be also not unique (two may coexist, one attracting the critical point and another attracting the kink point, see Sushko *et al.*, 2005, 2006). However, in our case the local maximum is exactly at the kink point, so that we cannot have bistability, also in I_{FG} the attracting set is necessarily unique. Differently, in the region (white region in Fig.2(b)) in which the absorbing interval J includes the three branches of map T, with a local maximum and a local minimum, it is possible to have bistability, that is, the existence of two different attracting sets (examples are given below).

In Fig.2(a) we highlight the result of the asymptotic behavior of the map with different colors, each color denotes a cycle of different period, while white regions correspond to the existence of chaotic intervals as attractors. The yellow regions in different tonalities show the regions in which one of the fixed points is globally attracting. Crossing the stability region of the fixed point k_F^*, as it follows from Proposition 3, the result can be an attracting cycle or a chaotic attractor, depending on the slope δ and similarly crossing the stability region of the fixed point k_H^* the result can be an attracting cycle or a chaotic attractor, depending on the two slopes δ and ε. In both cases the transition occurs inside an absorbing interval with two functions (colored regions in Fig.2(b)), so that, as commented above, the transition leads to a unique attractor.

As remarked in Proposition 3, we can have attracting cycles of period 2 with periodic points in different branches of the map. In Fig.2(a) different pink tonalities denote the existence of attracting period-2 cycles with different symbolic sequence (i.e. periodic points in different branches of the map). It is evident the region of the attracting 2-cycle marked FG, related to the flip bifurcation of k_G^*, that is the same region related to the border collision of the fixed point k_F^*, and also the region of the attracting 2-cycle marked GH, related to the flip bifurcation of k_G^*, that is the same region related to the border collision of the fixed point k_H^*. Moreover, we have a third region related to an attracting 2-cycle marked FH, that appears as persistence border collision of the attracting 2-cycle marked GH, but also as result of the degenerate flip bifurcation of the fixed point k_G^* at the particular point $P = (-1, k_P^*)$. In fact, in Proposition 3(a) we have commented the result of the flip bifurcation for $k^{FG} < k_P^*$ and $k^{FG} > k_P^*$, but not at $k^{FG} = k_P^*$. That point is particular, since it is a point of multiple bifurcations as in it three bifurcations are merging (the flip bifurcation of the fixed point k_G^* and two border collision curves commented below). As already mentioned, when the parameters are in point P, then the fixed point k_G^* is exactly in the middle of the related branch of definition of the function G, at the same distance from the two kink points, and that branch is filled with 2-cycles. In particular, the extrema belong to the 2-cycle with the kink points $\{k^{FG}, k^{GH}\}$, which attracts the points from outside the interval. It follows that this 2-cycle can be considered as a 2-cycle at its border collision, and it can be considered the merging with the kink points of a 2-cycle with periodic points in any two of the three different branches of map T. Stated differently, from the point P, decreasing δ, at a value $\delta < -1$ and close to -1, the result of

13

the bifurcation, depending on the value of the other parameters (in Fig.2(a) depending on k^{FG}) may be an attracting 2-cycle with periodic points in the branches F and H, or those marked FG or GH. It is possible to completely characterize also this bifurcation, that is, we can say exactly the result of the bifurcation, which depends on the other parameters. To this goal let us determine the existence region of the cycle FH.

Proposition 4 *Existence and bifurcations of the 2-cycle FH.*

The 2-cycle with points belonging to the branches F and H_l has periodic points given by $\{k_1, k_2\}$ with $k_1 = k_P^*$ given in (3.14) and $k_2 = C\sqrt{k_P^*}$, and it exists for $k_1 < k^{FG}$ and $k_2 > k^{GH}$.

The bifurcation occurring at $k_1 = k^{FG}$ corresponds to the border collision bifurcation curve

$$\psi_{FH}: \quad k^{FG} = k_P^* \tag{3.16}$$

leading, for $k^{FG} < k_P^*$, to attracting cycles or attracting chaotic intervals.

The bifurcation occurring at $k_2 = k^{GH}$ corresponds to the border collision bifurcation curve

$$\phi_{FH}: \quad k^{FG} = \left(\frac{1}{2\delta} \left(C - \sqrt{C^2 - 4\delta \overline{N_G}} \right) \right)^2 \tag{3.17}$$

where

$$\overline{N_G} = N_H + \frac{C(\varepsilon - \delta)}{2} \left(\varepsilon C + \sqrt{(\varepsilon C)^2 + 4N_H} \right) \tag{3.18}$$

leading, for $k^{FG} > C\sqrt{k_P^*}$, to a different attracting set (a 4-cycle in the case shown in Fig.2(a)).

Proof. We can determine the periodic points (k_1, k_2) of the 2-cycle FH considering $k_2 = F(k_1) = C\sqrt{k_1}$, then $k_1 = H_l(k_2) = \varepsilon k_2 + N_H$ leads to

$$k_1 - \varepsilon C\sqrt{k_1} - N_H = 0 \tag{3.19}$$

and thus to

$$k_1 = \frac{1}{4} \left(\varepsilon C + \sqrt{(\varepsilon C)^2 + 4N_H} \right)^2 \ (= k_P^*) \quad \text{and} \quad k_2 = \frac{C}{2} \left(\varepsilon C + \sqrt{(\varepsilon C)^2 + 4N_H} \right) \ (= C\sqrt{k_P^*}) \tag{3.20}$$

that exists for $k_1 < k^{FG}$ and $k_2 > k^{GH}$, and its stability follows from its eigenvalue λ, given by the product of the two derivatives $\lambda = F'(k_1)H_l' = F'(k_P^*)H_l'$ that is positive and $\lambda < 1$ since

$$\lambda = \frac{C\varepsilon}{2\sqrt{k_P^*}} = \frac{C\varepsilon}{\varepsilon C + \sqrt{(\varepsilon C)^2 + 4N_H}} = \frac{\varepsilon}{\varepsilon + \sqrt{\varepsilon^2 + 4N_H/C^2}} < 1 \tag{3.21}$$

this region is colored in dark pink in Fig.2(a).

Then, one bifurcation of this 2-cycle occurs when there is the merging of k_1 with the kink point k^{FG} and a second bifurcation occurs when there is the merging of k_2 with the kink point k^{GH}. So, the border collision bifurcation occurring at $k_1 = k^{FG}$ gives the bifurcation curve

$$\psi_{FH}: \quad k^{FG} = k_P^* \tag{3.22}$$

14

(In Fig.2(a) it corresponds to an horizontal straight line) and depending on the value of $\delta < -1$ this border collision can have different results. At the collision the periodic point $k_1 = k^{FG}$ is a fixed point of the second iterate of the map, so that the result of this border collision depends on the two slopes of map T^2 at the kink point k^{FG}. One slope (on the left side) is $\lambda = F'(k_P^*)H_l' < 1$ as given above in (3.21), and the other slope (on the right side) is $\mu = G'H' = \delta\varepsilon < 0$ (see an example in Fig.3(a)). For $\mu > -1$, (that is, $-\frac{1}{\varepsilon} < \delta < -1$) we have persistence of attracting fixed point for T^2, that corresponds to persistence of an attracting 2-cycle GH for T (see the border of the bifurcation curve ψ_{FH} related to this 2-cycle in Fig.2(a)). For $\mu < -1$ we certainly have an interval leading to an attracting 2-cycle for map T^2, that corresponds to an attracting 4-cycle of map T with symbolic sequence $FHGH$ (clearly visible in the azure region in Fig.2(a)), and so on, the values of the two slopes λ and μ determine the result of the bifurcation (by using the skew tent map as the border collision normal form).

The second border collision bifurcation of the 2-cycle FH occurs for $k_2 = k^{GH}$, that is

$$\frac{C}{2}\left(\varepsilon C + \sqrt{(\varepsilon C)^2 + 4N_H}\right) = \frac{1}{\varepsilon - \delta}[N_G - N_H]$$

(where $N_G = C\sqrt{k^{FG}} - \delta k^{FG}$) so that we have

$$C\sqrt{k^{FG}} - \delta k^{FG} = N_H + \frac{C(\varepsilon - \delta)}{2}\left(\varepsilon C + \sqrt{(\varepsilon C)^2 + 4N_H}\right) \tag{3.23}$$

Let $\overline{N_G} = N_H + \frac{C(\varepsilon - \delta)}{2}\left(\varepsilon C + \sqrt{(\varepsilon C)^2 + 4N_H}\right)$, from $\delta k^{FG} - C\sqrt{k^{FG}} + \overline{N_G} = 0$ we get the border collision bifurcation curve:

$$\phi_{FH}: \quad k^{FG} = \left(\frac{1}{2\delta}\left(C - \sqrt{C^2 - 4\delta\overline{N_G}}\right)\right)^2 \tag{3.24}$$

The result of this border collision of the 2-cycle FH depends on the two slopes at the colliding point $k_2 = k^{GH}$. On the left side of the kink point it is given by $F'(k_1)G'$ and on the right side by $F'(k_1)H_l'$. Since $F'(k_1) = F'(k_P^*)$, this second one is positive, $\lambda = F'(k_P^*)H_l' < 1$ as given in (3.21), and for the other one we have

$$F'(k_1)G' = F'(k_P^*)\delta = \frac{\delta}{\varepsilon + \sqrt{\varepsilon^2 + 4N_H/C^2}} < -1 \tag{3.25}$$

(see an example in Fig.3(b)). These two slopes, by using the skew tent map, determine the result of the bifurcation. In the case shown in Fig.2(a) this bifurcation leads to an attracting 2-cycle for map T^2, that corresponds to an attracting 4-cycle of map T with symbolic sequence $FHFG$ (clearly visible in the azure region in Fig.2(a), above the curve ϕ_{FH}).$\square$

An example is given in Fig.3 at $\delta = -3$ and the parameters as in Fig.2. In Fig.3(a) the border collision of the 2-cycle FH with the first kink point (point on the bifurcation curve (3.16)) and in Fig.3(b) with the second kink point (point on the bifurcation curve (3.17)). A peculiarity of this cycle is that at a fixed value of δ (varying only k^{FG}) the map changes shape while the periodic points of the 2-cycle are the same (being $k_1 = k_P^*$ and $k_2 = C\sqrt{k_P^*}$).
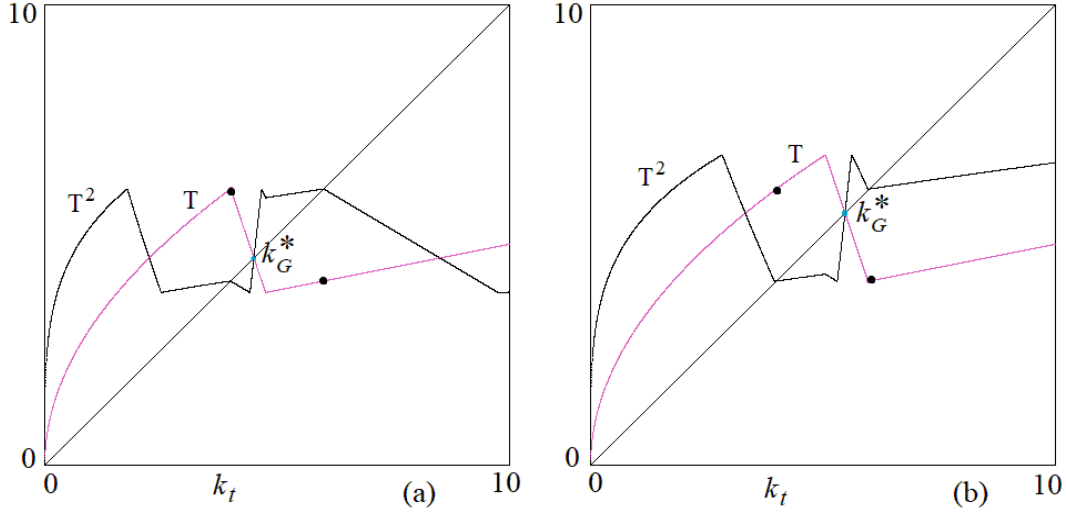
Fig.3 $\delta = -3$ and the parameters as in Fig.2. In (a) $k^{FG} = 4$. In (b) $k^{FG} = 5.05$

An immediate consequence of Proposition 4 is that a complete characterization of the degenerate flip bifurcation of the fixed point k_G^* at the particular point $P = (-1, k_P^*)$ is now possible. Considering a parameter value $\delta < -1$ and close to -1, then:

- for k^{FG} between the two curves ψ_{FH} and ϕ_{FH} the bifurcation leads to an attracting 2-cycle FH,

- for k^{FG} below the curve ψ_{FH} the bifurcation leads to an attracting 2-cycle GH,

- while for k^{FG} above the curve ϕ_{FH} the bifurcation leads to an attracting 2-cycle FG.

While the bifurcations associated with the 2-cycle FH are only the two border collisions, the other two kind of cycles of period 2 (FG and GH) bifurcated from the flip bifurcation of x_G^* can on their turn undergo a flip bifurcation, that is, we can also see a loss of stability due to a smooth flip bifurcation or due to a degenerate flip bifurcation, since the map is piecewise smooth, and the result of the bifurcation may be not the standard one (of period doubling). We prove the following

Proposition 5 *Bifurcations of the 2-cycles FG and GH.*
(i) *The 2-cycle FG with points belonging to the branches F and G undergoes a flip bifurcation crossing the curve*

$$f_{FG}: \quad \delta = \frac{-2}{3C^2}\left(k^{FG} + \sqrt{(k^{FG})^2 + 3C^3\sqrt{k^{FG}}}\right). \tag{3.26}$$

(ii) *The 2-cycle GH with points belonging to the branches G and H undergoes a degenerate flip bifurcation crossing the curve*

$$f_{GH}: \quad \varepsilon\delta = -1 \tag{3.27}$$

with different dynamic results depending on the parameters. (In the example of Fig.2 in the region with absorbing interval I_{GH} the bifurcation leads to four chaotic intervals, while in the region with absorbing interval J to an attracting 4-cycle)

16

Proof. The 2-cycle FG bifurcated from the flip bifurcation of k_G^* has periodic points (ξ_1, ξ_2) obtained considering $\xi_2 = F(\xi_1) = C\sqrt{\xi_1}$ and then $\xi_1 = G(\xi_2)$ leading to

$$\xi_1 - \delta C\sqrt{\xi_1} - N_G = 0 \tag{3.28}$$

so that

$$2\sqrt{\xi_1} = \delta C + \sqrt{(\delta C)^2 + 4N_G} \tag{3.29}$$

and the flip bifurcation occurs when the eigenvalue of the 2-cycle, given by the product of the two derivatives, is -1. This condition is $F'(\xi_1)G' = \frac{C}{2\sqrt{\xi_1}}\delta = -1$ leading to $2\sqrt{\xi_1} + C\delta = 0$. Substituting and computing we get

$$3C^2\delta^2 + 4\delta k^{FG} - 4C\sqrt{k^{FG}} = 0$$

and thus the flip bifurcation curve in (3.26), or equivalently:

$$f_{FG}: \quad k^{FG} = \frac{C^2}{4\delta^2}\left(1 - \sqrt{1 - 3\delta^3}\right)^2$$

Since in the present case the map is piecewise smooth, the fixed point of the second iterate of the map belongs to a smooth arc, so that the flip bifurcation may be a standard one, in general in smooth systems it can be subcritical or supercritical, and a degenerate case is also possible. In our case we leave this analysis to future work. However, a few examples suggest that it is a degenerate bifurcation. At the flip bifurcation value the map has four segments filled with cycles of period 4, bounded by the periodic points of the 2-cycle (connecting two segments), the kink point closest to the 2-cycle and its three images, that is, the fourth iterate of the map, T^4, has two segments exactly on the diagonal, filled with periodic points and the external kink point belongs to a 4-cycle at its border collision. To determine the result of the border collision we use the skew tent map as border collision normal form, considering the two slopes of the map T^4 at this kink point.

In our system this result differs depending on the region to which the parameters belong. That is, the result depends on the kind of existing absorbing interval. For parameters in the region with interval I_{FG}, in which only the branches F and G are involved (gray region in Fig.2(b)), the two slopes are both higher than 1 in absolute value (an example is shown in Fig.4(a)), and the result is 4 chaotic intervals, bounded by the images of the kink point k^{FG} (an example is shown in Fig.4(b)). The symbolic sequences involved in this chaotic set are the occurrence of $FGFG$ and $FGGG$ in an unpredictable way. Differently, for parameter in the region with absorbing interval J (white region in Fig.2(b)), even if only the branches F and G are involved, the kink point on the boundary of the segments filled with 4-cycles is k^{GH} (an example is shown in Fig.5(a)) and one slope of map T^4 at this kink point is smaller than 1 and the result is an attracting 4-cycle with periodic points $FGFH$ (an example is shown in Fig.5(b)).

17
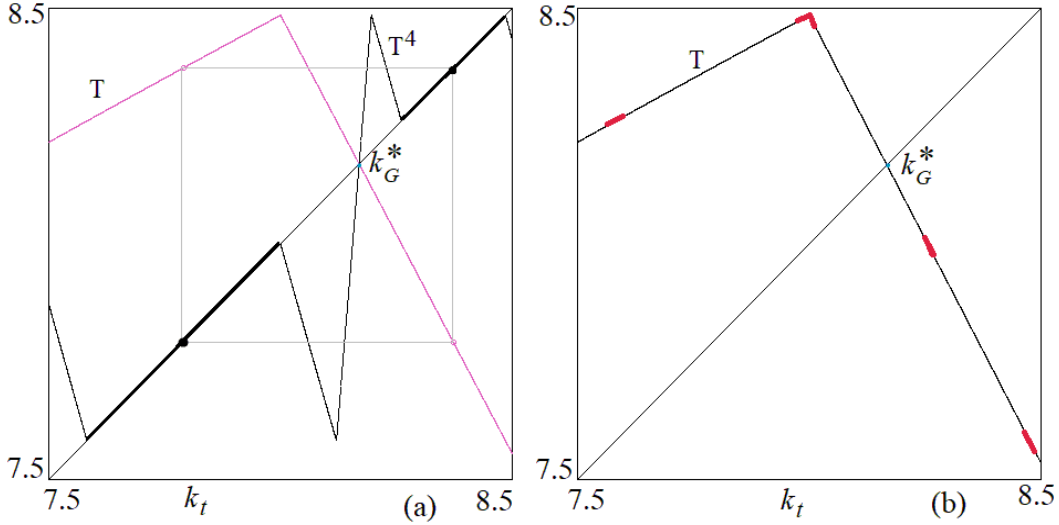
Fig.4 $k^{FG} = 8$, and the parameters as in Fig.2. In (a) $\delta = -1.860758$, on the diagonal are evidenced segments filled with 4-cycles; in (b) $\delta = -1.9$ there are four chaotic intervals evidenced in red
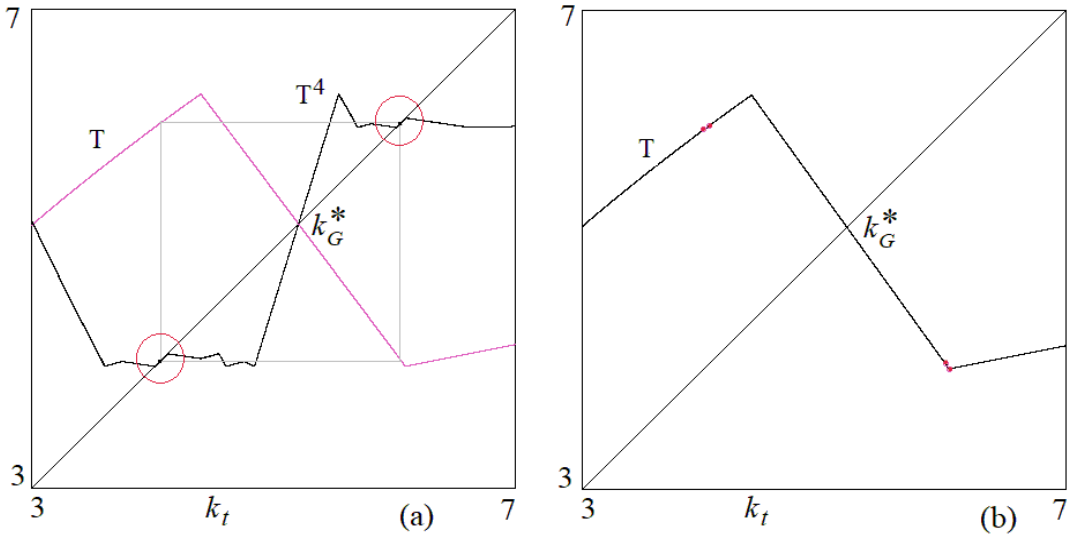
Fig.5 $k^{FG} = 4.4$, and the parameters as in Fig.2. In (a) $\delta = -1.344995$, on the diagonal the circles are evidencing segments filled with 4-cycles; in (b) $\delta = -1.4$, a 4-cycle is the attracting set, evidenced by the red points

The 2-cycle GH bifurcated from the flip bifurcation of k_G^* has periodic points (η_1, η_2) obtained considering $\eta_2 = G(\eta_1) = \delta\eta_1 + N_G$ then $\eta_1 = H_l(\eta_2)$ leads to

$$\eta_1 = \varepsilon(\delta\eta_1 + N_G) + N_H \tag{3.30}$$

so that

$$\eta_1 = \frac{\varepsilon N_G + N_H}{1 - \varepsilon\delta} \quad , \quad \eta_2 = \frac{N_G + \delta N_H}{1 - \varepsilon\delta} \tag{3.31}$$

The flip bifurcation occurs when the product of the two derivatives is -1, that is:

$$f_{GH}: \quad \varepsilon\delta = -1$$

18

In Fig.2(a) $\delta = -1/\varepsilon = -5$ is a vertical segment. Since the two branches with the periodic points of the 2-cycle are linear, this flip bifurcation is necessarily degenerate.

At the bifurcation value the map has two segments including the 2-cycle that are filled with cycles of period 4, and the external one has a point in one kink point, the closest to the 2-cycle, which may be either k^{FG} or k^{GH}.

When the parameters belong to the area in which the map is restricted to the absorbing interval I_{GH} (light blue region in Fig.2(b)), then the result of the degenerate flip bifurcation of the 2-cycle involves the kink point k^{GH} and the bifurcation leads to 4 chaotic intervals (an example is shown in Fig.6(a)). Differently, when the parameters belong to the area in which the map is restricted to the absorbing interval J (white region in Fig.2(b)), then the kink point k^{FG} is involved and this bifurcation leads to a period doubling, an attracting 4-cycle with symbolic sequence $FHGH$ exists after the bifurcation (an example is shown in Fig.6(b)).□
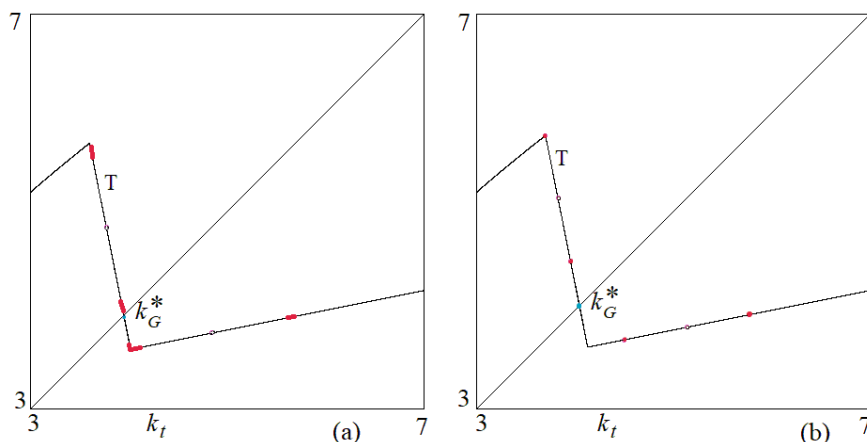
Fig.6 $\delta = -5.01$, and the parameters as in Fig.2. In (a) $k^{FG} = 3.6$, there are four chaotic intervals evidenced in red; in (b) $k^{FG} = 3.7$, a 4-cycle $FHGH$ is the attracting set, evidenced by the red points

As remarked above, in the parameter space there exists a wide region related to a bimodal map, involving all the three functions. We do not present a comprehensive analysis of this region, but highlight two properties that are interesting from an economic point of view:

1. In this region we have attracting cycles as well as attracting chaotic intervals. An example of the possible trajectories is shown in the one-dimensional bifurcation diagram as a function of δ in Fig.7
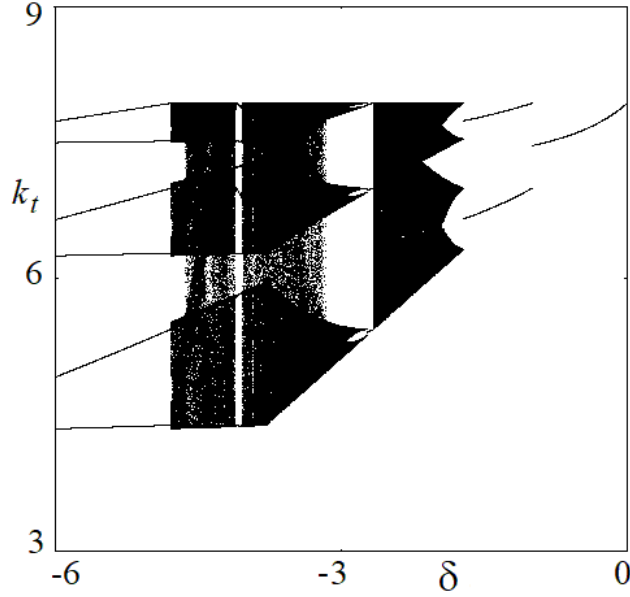
Fig.7 $k^{FG} = 7$ and the parameters as in Fig.2

2. Clearly, in this parameter region, inside the absorbing interval J it is possible to have coexistence of attractors. An example is shown in Fig.8.
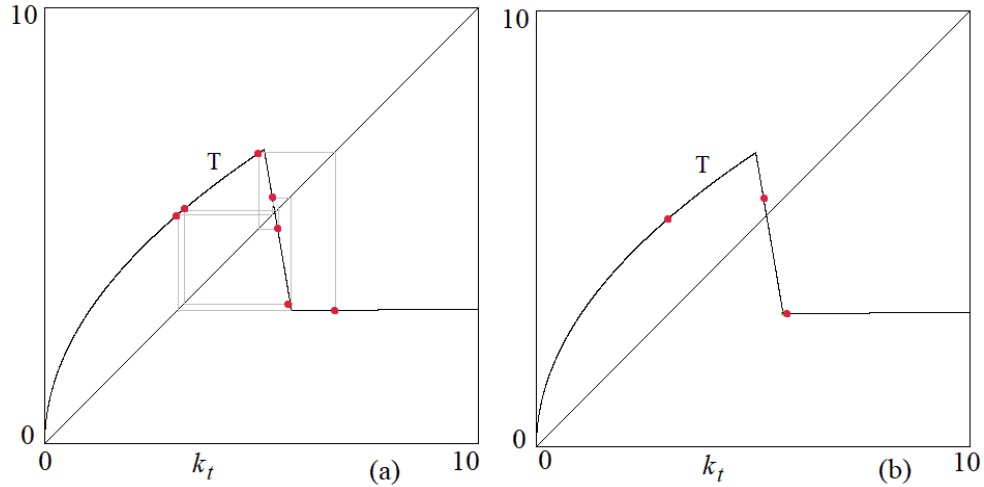
Fig.8 $k^{FG} = 5.06$, $\delta = -5.85$ and the parameters as in Fig.2, there are coexisting attracting cycles, evidenced by the red points. In (a) there is an attracting 7-cycle $FGGFGFH$; in (b) a 3-cycle FGH is the attracting set

4. Discussion of Results and Final Remarks

We presented a model in the spirit of Matsuyama's model of endogenous financial cycles (Matsuyama *et al.*, 2016), which we augmented by agents's heterogeneity. We showed that in the resulting model old agents have two margins for adjusting their financial decisions: first they decide whether to become entrepreneur or not; second, they decide

on the amount to invest in entrepreneurial projects. The corresponding map has three branches that correspond to three different regimes with respect to the investments in bad projects: on a first branch, bad projects are not available (and all investment goes to entrepreneurial, good projects); on a second, middle branch, investment in bad projects becomes increasingly available, and, finally, on a third branch, investment in bad projects is not limited anymore. We showed that - because of heterogeneity - the third branch is upward sloping. We specified the functional forms, linearized two branches, and described analytically important properties of the implied dynamics. We paid particular attention to the nature of business cycles, commenting not only on the movement of capital and output per capita, but also on the length of the business cycles and in particular also on the pattern of regime switches that are involved. In presenting the results, we focused on their dependence upon the availability of bad projects, i.e. on the parameter k^{FG} (the lower k^{FG}, the sooner bad projects become available) and δ (the lower δ the quicker the availability of bad projects increases with an increase in k_t).

From an economic point of view, we would like to highlight the following results:

1. The map involves three fixed points (one on each branch characterized by a specific regime) and we analytically describe the parameter space, in which these fixed points are stable. For low (high) values of k^{FG}, the dynamics converges to the fixed point in which investment in bad projects is unlimited (not available). For intermediate values of k^{FG} and for values of δ between 0 and -1, the dynamics converges to the fixed point, in which investment in bad projects are available, but limited.

2. We gave a full description of how the fixed points bifurcate into period-2 cycles. Importantly, we are able to analytically describe the parameter spaces with different symbolic sequences on the cycles (involving economically different regime switches): All two cycles occur for $\delta < -1$. If bad projects become available at a low threshold k^{FG}, the cycle fluctuates between constrained and unconstrained investment in bad projects (which corresponds to the symbolic sequence GH). For intermediate values of k^{FG} the dynamics switches between unconstrained and no investment in bad projects (symbolic sequence FH), whereas for high values of k^{FG} the cycles are between constrained and no investment in bad projects (symbolic sequence FG). Thus, we are able to describe analytically regime switches over the cycle; as well as how the nature of period-2 cycles changes with varying parameters.

3. We have also fully described how the FH cycle bifurcates (Proposition 4). It does not only bifurcate into period-2 cycles with a different symbolic sequence (commented upon in the previous paragraph); in addition, we gave parameter conditions for which it bifurcates into period-4 cycles. Interestingly enough, these period-4 cycles may exhibit two different symbolic sequences: For a lower value of k^{FG} a $FHGH$ period-4 cycle appears, on which the cycle starts with no investment in bad projects, goes then into the regime with unconstrained investment in bad projects, enters the regime with constrained investment in bad projects and finally the regime with unconstrained investment in bad projects; then the cycle starts over again. Instead, for a higher value of k^{FG} a $FHFG$ period-4 cycle appears, on which the cycle starts

21

with no investment in bad projects, goes then into the regime with unconstrained investment in bad projects, returns to the regime with no investment in bad projects and finally enters the regime with constrained investment in bad projects; then the cycle starts over again. Again, our model provides not only conditions for the change in cycle length, but also conditions on the nature of regime switches on cycles with the same cycle length.

4. The model is highly stylized and therefore it is difficult to take it directly to the data. However, it describes a mechanism that might be able to generate cyclical patterns similar to the ones found in data. From an economic perspective, it is interesting to note that the model does not only describe regular cycles of low periodicity that may appear as a not fully convincing description of reality (which always involves irregular fluctuations). As shown, the period-2 cycles may not only bifurcate into regular period-4 cycles, but also into attractors involving four chaotic intervals (see Proposition 5, on the bifurcations of the GH and the FG cycles, and Fig.4(b) and Fig.6(a) for examples of the attractors; and the one-dimensional bifurcation diagram in Fig.7, in which the attractors involving chaotic intervals are clearly visible). The dynamics on these attractors with four chaotic intervals resembles an irregular period-four cycle, which is a much more plausible pattern in an economic context.

5. Our model also involves coexisting attractors with totally different symbolic sequences. Fig.8 shows coexistence of a period-three cycle FGH with a period-seven cycle, which - notably enough - does NOT involve the sequence FGH. The nature of regime switches and their sequence is sensitive upon initial conditions and may thus change abruptly after a shock.

6. Importantly, we would like to highlight the role of heterogeneity in our model. Without heterogeneity, the branch $H_l(k_t)$ is horizontal, $\varepsilon = 0$ holds.

   First observe, the dynamics is not affected by heterogeneity, where I_{FG} is the absorbing interval (i.e. where the map only involves the branches $F(k_t)$ and $G(k_t)$, see the gray area in Fig.2(b)) and the slope of the branch $H_l(k_t)$ is not involved.

   Second, in the other regions the dynamics involves also the third branch. Without heterogeneity it is flat and all cycles are superstable, which also implies that attractors involving chaotic intervals are not possible. This holds also for the Flip bifurcation of the GH cycle. Introducing heterogeneity thus increases the economic plausibility of the implied dynamic patterns.

7. Finally, note that our analysis also leads into various policy questions. It highlights the importance of financial institutions for the generation of business cycles, for creating volatility, and shows the fragility of economic stability. Small institutional shocks may drastically change the economic development. Our analysis also reveals additional challenges for economic policy. It does not suffice to observe the development of total output and income, since business cycles similar in income development may actually involve quite different pattern of regime switches and thus call for different policy responses. In addition, introducing heterogeneity also allows to study

the impact of business cycles on occupational choice and income inequality, thus opening up further policy fields. However, for digging deeper into these questions our analytic approach has to be complemented by numerical analyses.

We leave this and other applications to further research.

References

Avrutin V., L. Gardini, Sushko I, Tramontana F. (2019). Continuous and Discontinuous Piecewise Smooth One-Dimensional Maps: Invariant Sets and Bifurcation structures. World Scientific, Singapore. https://doi.org/10.1142/8285.

Bougheas, S., Commendatore, P., Gardini, L., Kubin, I. (2022). Financial development, cycles and income inequality in a model with good and bad projects. *CES-ifo Working Paper* No. 10135, University of Munich.

Kubin, I., Zörner, T., Gardini, L. & Commendatore, P. (2019). A credit cycle model with market sentiments. *Structural Change and Economic Dynamics,* 50, 159-174.

Kubin, I., Zörner, T. (2021). Credit cycles, human capital and the distribution of income. *Journal of Economic Behavior and Organization,* 183, 954-975.

Matsuyama, K. (2013). The good, the bad, and the ugly: An inquiry into the causes and nature of credit cycles. *Theoretical Economics,* 8, 623-651.

Matsuyama, K., Sushko, I., Gardini, L. (2016). Revisiting the model of credit cycles with good and bad projects. *Journal of Economic Theory,* 163, 525-556.

Sushko I., Gardini L. (2010). Degenerate bifurcations and border collisions in piecewise smooth 1D and 2D maps. *Int. J. Bif. Chaos,* 20, 2045-2070.

Sushko I, Avrutin V., Gardini L. (2015). Bifurcation structure in the skew tent map and its application as a border collision normal form. *Journal of Difference Equations and Applications.* DOI: 10.1080/10236198.2015.1113273

Sushko I., Agliari A., Gardini L. (2005). Bistability and bifurcation curves for a unimodal piecewise smooth map. *Discrete and Continuous Dynamical Systems*, Serie B, Vol.5, N.3, 881-897.

Sushko I., Agliari A., Gardini L. (2006). Bifurcation structure of parameter plane for a family of unimodal piecewise smooth maps: border-collision bifurcation curves. *Chaos Solitons & Fractals,* 29(3), 756-770.

Declarations